Published by :
http://www.ijert.org

International Journal of Engineering Research & Technology (IJERT)
ISSN: 2278-0181
Vol. 5 Issue 02, February-2016

Dynamic Performance of Continuously Variable Transmission Device

A. A. Metwally [1]
Student, ME
Arab Academy for Science and Technology and Maritime Transport
Department of Mech. Eng.
Latakia, Syria

E. Saber[2]
Professor,
Arab Academy for Science and Technology and Maritime Transport.
Department of Mech. Eng.
Latakia, Syria

E. M. Attia[3]
Ass. Prof,
Arab Academy for Science and Technology and Maritime transport
Department of Mech. Eng.
Latakia, Syria

Abstract **- The steeples shifting pattern of the transmission provides a very comfortable drive, as well as having full vehicle performance, available at any time .This type of transmission can realize many advantages such as, low engine revolutions at constant speeds, improved emission control/fuel consumption and low noise vibration and harshness levels. In addition it can achieve smooth acceleration and flexible driving on mountain road. This work study the dynamic performance of the main mechanical components of CVT used for power transmission. A reduced model for hybrid small vehicle is introduced and the relations describing the drive line model follow from the equations of motions was derived. Effect of different acceleration on dynamic response of output torque and linear velocity of scooter was studied. Also a computer-operated and programmed for the different functions of that CVT is used. A Simulink program using MATLAB software package was used for solving the equations of motions.**

Keywords: Continuous, CVT, Transmission, dynamic, Models, Speed, Variable

I - INTRODUCTION

Continuously variable transmission (CVT), as its name suggests, continuously varies the gear ratio. A low gear (low ratio) makes it easier to pull away from a rest position, the drive pulley diameter being relatively small, while the driven pulley diameter is large by comparison. The drive belt is possible to select a higher ratio by increasing the diameter of the drive pulley. As acceleration takes place it become possible to select a higher ratio by increasing the diameter of the drive pulley while, at the same time, decreasing the diameter of the driven pulley. This degree of change can be controlled to ensure that the most suitable ratio is provided. Ramnath [1] studied about the development of high torque C.V.T. fluids, because the efficient transmission of torque requires relatively high steel-on-steel friction with minimal wear between the belt or chain & the pulley. He also talked about the tests achieved on different types of fluids & the degree of viscosity of each one.Van de Meerakker, et.al.[2] investigated the design of an electromechanical ratio & clamping force actuator for a metal V-Belt type C.V.T., they talked about the conventional belt type C.V.T. & the hydraulic power loss, also referred to the alternatives. The belt type C.V.T. has two parallel shafts with pulleys. Torque is transmitted between the shafts by means of a segmented steel V-Belt, which runs between the pulleys. Most belt type CVT's on the market are actuated hydraulically. Fujita et.al [3] introduced the structure of a new CVT system equipped with a dry hybrid V-Belt. The belt has a structure of a pair of tension bands inserted in many H-shaped blocks. The core of the block is made of high strength aluminum alloys supporting a high transverse load from pulleys. The core is covered with phenol resin giving the blocks a proper frictional coefficient with the pulleys. No lubrication is needed. Which realize excellent transmitting efficiency in the CVT system. Aramid cords supporting belt tension lies at the center of the tension bands. Heat resisting rubber material made of hydrogenated nitrile rubber surrounds the aramid chords. Bonsen et.al.[4] studied the control-oriented identification of an electromechanically actuated metal V-Belt CVT. The torque delivered by the engine is obtained from measured engine data, depending on engine speed & throttle position. The torque converter (TC) is modeled using an impeller torque at the engine body & a turbine torque at the primary shaft of the CVT. These torques are calculated using (TC) characteristics depending on the engine speed & (TC) speed ratio. The wheels of the vehicle are connected to the output shaft of the final reduction using a torsion spring, which models the combined stiffness of both the drive shafts. Hendriks, et.al. [5] studied the metal belt-CVT's based on the theories of Euler can attain higher 'power-density-values' which are drives'. In the fixed ratio mechanical transmission, the cylindrical gears with spur or helical teeth attain the highest compactness values followed by roller or toothed chain. Among the CVT's the metal V-belt CVT attains the highest compactness values when compared to traction drive. The V-belt consists of a number of thin, flat tension bands of steel, which have a very narrow mutual tolerance. Kato et.al. [6] Studied the torque capacity of belt CVT's. they studied the structure of the metal belt, the V-shaped input & output pulleys, the torque which is transmitted by the compressive force between the elements, produced by the friction force

International Journal of Engineering Research & Technology (IJERT)
ISSN: 2278-0181
Vol. 5 Issue 02, February-2016

acting between the sides of the elements & the cone-shaped pulley forces. Naishi et.al. [7] studied the match design method of the cone discs & flexible members; this is the belt-type or chain-type CVT. In the transmission process the inner cone surface contacts with the parts of the flexible members which is outside the point of M & the outer cone surface contacts with the parts inside the point of M. Sugano et.al.[8] worked on the development of new generation of belt CVTs with high torque capacity for front-drive cars. This new generation includes three belt CVTs, ranging in torque capacity from 100 to 350 Nm. These new-generation CVTs are developed with the aim of achieving a more compact design, lighter weight and a wider ratio range. To improve the product appeal of these new generation CVTs, a super ultra-flat torque converter was developed along with reducing the diameter of the primary pulley. Fujii et.al. [9] studied the distribution of block compression force on the driving and driven pulleys were measured using a tiny load-cell inserted between two blocks and a telemeter system, under several constant speed ratios. Kanehara et.al.[10] studied other forces simultaneously acting on a block at steady states were measured using newly developed devised blocks. These forces are frictional force between blocks and rings, normal force between blocks and pulleys, frictional forces between blocks and pulleys in radial and tangential directions.By measuring six forces components acting on the blocks of a metal pushing V-belt at transitional states Takashi Kitagawa, Fujii, et.al[11] found that at transitional states, the distribution of forces acting on the blocks are foundationally different in shape from the force distributions at steady states. Weather the pulley is a driving or driven, the behavior of the blocks at transitional states is affected by the transition of width of pulley groove, that of the belt pitch diameter. Kobayashi, et.al. [12] Studied the analysis of the mechanism causing the micro slip characteristic of a metal CVT belt during torque transmission, focusing on the gap distribution between the elements. Yamaguchi et.al.[13] described the development of a detection system of maximum force for a metal belt type CVT. Van Drogen et.al. [14] Described a method to select fluids for push belt CVT application. The test method comprises full load testing in several ratios in which durability and functionality related push belt CVT items are being examined. Gunsing et.al. [15] Described the steps taken to isolate the noise source and eliminate it. Initial investigation revealed that the scratch phenomenon could be avoided by using an alternative transmission fluid. During this work, it was found that existing automatic transmission fluid (ATF) specifications did not necessarily contain performance requirements that describe a particular fluid's suitability for CVT application. Okubu et.al. [16] Developed an implicit finite element to accurately analyze the power transmitting mechanisms of CVT using a dry hybrid V-belt. The calculated results showed that the blocks were subjected to an over-load due to the pulley flange tilting. Nakazawa et.al. [17] Described the performance of the CVT fluid in lab-scale tests and an endurance test of the CVT unit. In order to realize high torque transmission between a steel belt and pulleys, high friction between metal/metal is required with normal wear. A CVT fluid was selected and further tests showed it to give high and stable coefficients of friction and low level of wear. Mölle [18] presented a new adaptive controller layout for chain converters for universal use in different applications and set-ups. Based on the control structure chosen for synchronization of the claw couplings of a chain converter type during range shifts, a universal control layout was developed. Both the conventional clamping system for the based chain converter and a newly developed pressure controlled clamping system were taken into account. In an effort to improve the Continuously Variable Transmission and evaluate its performance with different modifications, Frank [19] redesigned a conventional CVT to incorporate an energy efficient Servo Hydraulic Control (SHC) system and to substitute a different torque transmitting element, a Gear Chain Industry (GCI) chain for the Van Doorne Transmissie (VDT/Bosch) belt.Tran et.al.[20] developed a new maraging steel, that will be applied in the new phase 7 push-belt design with a planned production start at the end of 2005. This phase 7 push-belt design enables further extension of the current CVT application range to higher upper class applications with 200kw of engine power. Tani et.al. [21] Reported the development of a simulation model that can predict fundamental characteristics of a metal V-belt CVT with useful accuracy within a reasonable amount of calculation time. The model uses a combination of load analysis based on equilibrium equations and slip velocity analysis based on the evaluation of the pulley displacement. Srivastava [22] focused on developing models to understand the micro slip behavior and to define an operating regime of a metal pushing V-belt CVT. Slip is modeled on the basis of gap redistribution between the elements.

International Journal of Engineering Research & Technology (IJERT)
ISSN: 2278-0181
Vol. 5 Issue 02, February-2016

II. MATHEMATICAL MODELING

Applying Dalamber't principle for flywheel and primary pulley, the following equation is obtained

$$\boldsymbol{j_f\ddot{\varphi}_f = T_e - b_f\dot{\varphi}_f - T_p} \qquad (1)$$

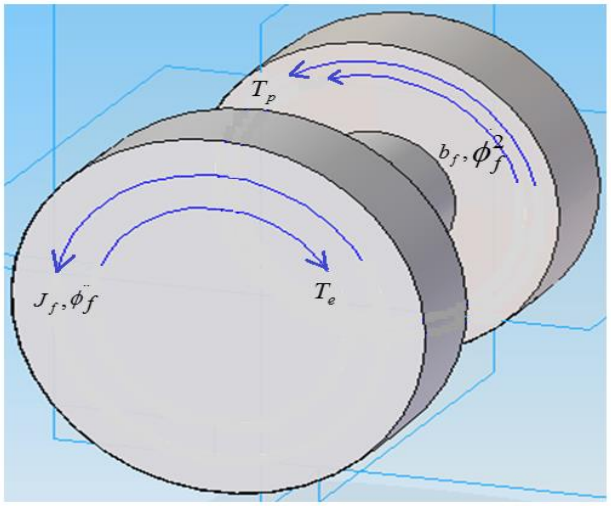

Figure 1: Loads acting on flywheel and primary pulley

Applying Dalamber't principle for the vehicle and secondary pulley

$$\boldsymbol{T_s = k_t(\varphi_s - \varphi_v) + c_t(\dot{\varphi}_s - \dot{\varphi}_v)} \qquad (2)$$

Where,

T_e is the engine torque

T_p is the torque of the primary pulley

T_s is the torque of the secondary pulley

ϕ_f , ϕ_s and ϕ_p are the twist angles of flywheel , secondary pulley and primary pulley

$\dot{\phi}_f$, $\dot{\phi}_p$ and $\dot{\phi}_s$ are the angular velocities of flywheel , primary pulley and secondary pulley

$\ddot{\phi}_f$, $\ddot{\phi}_p$ and $\ddot{\phi}_s$ are the angular accelerations of flywheel , primary pulley and secondary pulley

The deformation ε is defined as the relative angle over the torsion spring which is connected between secondary pulley and vehicle wheel. $\boldsymbol{\varepsilon = \varphi_s - \varphi_v}$ (3)

$\dot{\varepsilon}$ is the relative angular velocity over the torsion spring

$$\boldsymbol{\dot{\varepsilon} = \dot{\varphi}_s - \dot{\varphi}_v} \qquad (4)$$

The torque of the secondary pulley can be put in the form,

$$\boldsymbol{T_s = k_t\varepsilon + c_t\dot{\varepsilon}} \qquad (5)$$

As mentioned before the CVT ratio is defined by i and is in the form,

$$\boldsymbol{i = \frac{\dot{\varphi}_s}{\dot{\varphi}_p}} \qquad (6)$$

The efficiency of CVT is defined by η and can be formulated by,

$$\boldsymbol{\eta = \frac{i * T_s}{T_p}} \qquad (7)$$

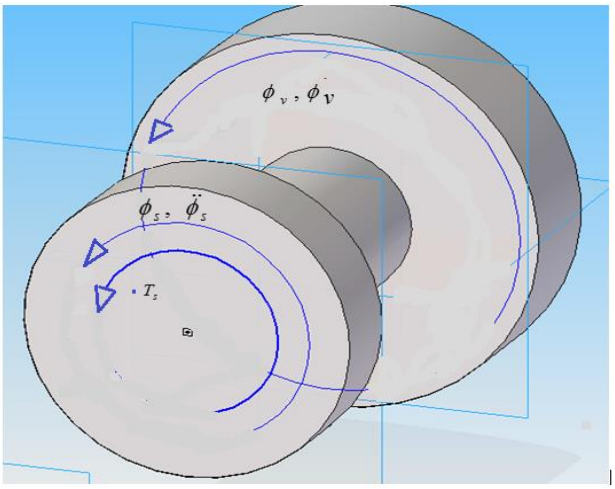

Figure 2: Vehicle and secondary pulley loads model

The torque of the primary pulley is formulated as,

$$\boldsymbol{T_p = \frac{i}{\eta}(k_t\varepsilon + c_t\dot{\varepsilon})} \qquad (8)$$

Using equations 1 and 8 the following equation can be obtained

$$\boldsymbol{j_f\ddot{\varphi}_f = T_e - b_f\dot{\varphi}_f^2 - \frac{i}{\eta}(k_t\varepsilon + c_t\dot{\varepsilon})} \qquad (9)$$

Applying Dalamber't method for secondary pulley and vehicle wheel

$$\boldsymbol{j_v\ddot{\varphi}_v = k_t\varepsilon + c_t\dot{\varepsilon} - b_v\dot{\varphi}_v^2 - T_{ex}} \qquad (10)$$

Where, T_{ex} is the external torque acting on the vehicle

The relative angular velocity over the torsion spring can be formulated as,

$$\boldsymbol{\dot{\varepsilon} = i\dot{\varphi}_f - \dot{\varphi}_v} \qquad (11)$$

And the relative angular acceleration over the torsion spring is,

International Journal of Engineering Research & Technology (IJERT)
ISSN: 2278-0181
Vol. 5 Issue 02, February-2016

$$\ddot{\varepsilon} = i\ddot{\varphi}_f + \dot{\varphi}_f \frac{di}{dt} - \ddot{\varphi}_v \quad (12)$$

Where, $\ddot{\varphi}_f$, $\ddot{\varphi}_v$ are the angular velocity of the fly wheel and vehicle respectively

$$\ddot{\varphi}_f = \frac{(\ddot{\varepsilon} - \dot{\varphi}_f \frac{di}{dt} + \ddot{\varphi}_v)}{i} \quad (13)$$

Using equation 13 into equation 9 the following equation is formulated,

$$j_f\ddot{\varphi}_v = i\left(T_e - b_f\dot{\varphi}_f^2 - \frac{i}{\eta}(k_t\varepsilon + c_t\dot{\varepsilon})\right) - j_f\ddot{\varepsilon} + j_f\dot{\varphi}_f\frac{di}{dt} \quad (14)$$

Divide equation 14 by equation 10 then,

$$j_f\ddot{\varepsilon} = -(k_t\varepsilon + c_t\dot{\varepsilon})\left[\frac{i^2}{\eta} + \frac{j_f}{j_v}\right] - b_f i\dot{\varphi}_f^2 + iT_e + \frac{j_f}{j_v}T_{ex} + \frac{j_f}{j_v}b_v(i\dot{\varphi}_f - \dot{\varepsilon})^2 + j_f\dot{\varphi}_f\frac{di}{dt} \quad (15)$$

A. *Geometrical and kinematic aspects:*

In order to obtain a desired rate of ratio change, a certain axial velocity is required. This velocity is proportional to control signal required to move the moving part of pulley axially. the relations for the required axial velocity can be derived from the ratio and the required rate of ratio change of CVT. It is possible to relate the running radii r_p and r_s on the primary respectively on the secondary pulley to the CVT ratio i. using the angle δ yields. It is possible to relate the relation between the running radii r_p and r_s of CVT on angle δ see figure 3.

B. Speed ratio change

To obtain a desired rate of ratio change, a certain axial pulley sheave velocity is required. The velocity depends on the signal from control to move the moving part of pulley axially see Figure 4.

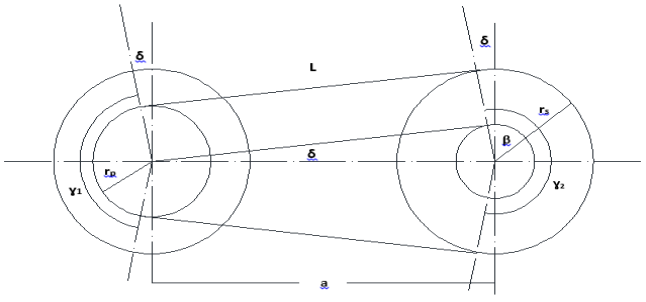

Fig. 3 : CVT geometry

L is the length of belt,

γ_1 is the contact angle for the driver pulley,

γ_2 is the contact angle for the driven pulley,

$$\gamma_1 = \pi - 2\delta \quad (16)$$

$$\gamma_2 = \pi + 2\delta \quad (17)$$

$$(\pi - 2\delta)r_p + (\pi + 2\delta)r_s + 2a = L \quad (18)$$

$$r_s - r_p a\sin\delta \quad (19)$$

$$i = \frac{r_p}{r_s} \quad (20)$$

$$\beta = \frac{\pi}{2} - \delta \quad (21)$$

Then

$$(r_s - r_p) = a\cos\beta = a\cos\left(\frac{\pi}{2} - \delta\right) \quad (22)$$

From 18

$$(\pi - 2\delta)ir_s + (\pi + 2\delta)r_s + 2a\cos\delta = L \quad (23)$$

From eq. 24

$$\left[\left(\frac{\pi}{2} - \delta\right)i + \left(\frac{\pi}{2} + \delta\right)\right]r_s = \frac{L}{2} - a\cos\delta \quad (24)$$

then

$$\left[\left(\frac{\pi}{2} - \delta\right)i + \left(\frac{\pi}{2} + \delta\right)\right]r_s = a\left[\frac{L}{2a} - \cos\delta\right] \quad (25)$$

From eq. 19

$$(1 - i)r_s = a\sin\delta \quad (26)$$

$$r_s = \frac{a\sin\delta}{1 - i} \quad (27)$$

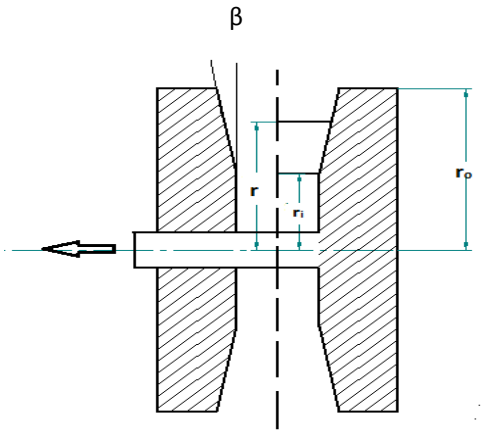

Fig. 4: Variation of pulley radius during motion

International Journal of Engineering Research & Technology (IJERT)
ISSN: 2278-0181
Vol. 5 Issue 02, February-2016

From eq. 25 and 27

$$\left[\left(\frac{\pi}{2}-\delta\right)i+\left(\frac{\pi}{2}+\delta\right)\right]a\sin\delta = a(1-i)\left[\frac{L}{2a}-\cos\delta\right] \quad (28)$$

Then

$$(1-i)\cos\delta+\left[\left(\frac{\pi}{2}+\delta\right)+i\left(\frac{\pi}{2}-\delta\right)\right]\sin\delta = (1-i)\frac{L}{2a} \quad (29)$$

Linear sheave velocity for primary and secondary pulley

$$x = (r - r_i)\tan\alpha \quad (30)$$

$$v_p = 2\dot{x} \quad (31)$$

$$v_p = 2(\dot{r}_p)\tan\alpha \quad (32)$$

$$v_s = 2(\dot{r}_s)\tan\alpha \quad (33)$$

To find $\dot{r}_p, \dot{r}_s$, from 25

$$\left[\left(\frac{\pi}{2}-\delta\right)i+\left(\frac{\pi}{2}+\delta\right)\right]\dot{r}_s = -\left(\frac{\pi}{2}-\delta\right)r_s\frac{di}{dt} \quad (34)$$

As $r_p = i\,r_s$ (35)

$$\dot{r}_p = i\dot{r}_s + r_s\frac{di}{dt} \quad (36)$$

$$\dot{r}_s = \frac{1}{i}\left[\dot{r}_p - r_s\frac{di}{dt}\right] \quad (37)$$

$$\frac{1}{i}\left[\left(\frac{\pi}{2}-\delta\right)i+\left(\frac{\pi}{2}+\delta\right)\right]\left[\dot{r}_p - r_s\frac{di}{dt}\right] = -\left(\frac{\pi}{2}-\delta\right)r_s\frac{di}{dt} \quad (38)$$

$$\left[\left(\frac{\pi}{2}-\delta\right)i+\left(\frac{\pi}{2}+\delta\right)\right]\left[\dot{r}_p - r_s\frac{di}{dt}\right] = -i\left(\frac{\pi}{2}-\delta\right)r_s\frac{di}{dt} \quad (39)$$

$$\left[\left(\frac{\pi}{2}-\delta\right)i+\left(\frac{\pi}{2}+\delta\right)\right]\dot{r}_p - i\left(\frac{\pi}{2}-\delta\right)r_s\frac{di}{dt} + r_s i\left(\frac{\pi}{2}\delta\right)\frac{di}{dt}r_s\left(\frac{\pi}{2}\delta\right)\frac{di}{dt} \quad (40)$$

$$\left[\left(\frac{\pi}{2}-\delta\right)i+\left(\frac{\pi}{2}+\delta\right)\right]\dot{r}_p = \left(\frac{\pi}{2}+\delta\right)r_s\frac{di}{dt} \quad (41)$$

To find the rate of radius changes for primary and secondary pulley apply the following procedures.

-Assume speed ratio i

-Find δ from equation 22

-Find r_s from equation 23

-Find r_p from equation 19

-Find $\dot{r}_s$ from equation 34

-Determine $\dot{r}_p$ from 36

III. RESULTS AND DISSCUSSIONS

In this work the results are concerned on low velocity mode, and data of electric scooter is used as a model for the results obtained in this section.

Table 1 : Model parameters

variable	Description	Initial value	Units
Power	Maximum power	2.2	Kw
A	Center distance	0.275	m
L	Length	0.8954	m
N	Speed of motion	3000	rpm
T_{max}	Maximum torque	11	N.m
W	Load capacity	150	Kg
d_w	Tyre (vacuum tyre)	0.035 – 0.1	m
η	Efficiency	0.75	-
kt	Torsional stiffness	320	N.m/rad
θ_t	Twist angle	5	rad
N_1	Speed of primary pulley	3000	rpm
N_2	Speed of secondary pulley	1000	rpm
V_s	Velocity of scooter	60	Km/h
m_s	Total mass of scooter	225	Kg
j_f	Moment of inertia of fly wheel	0.7	$Kg.m^2$
j_s	Moment of inertia of scooter	7.5	$Kg.m^2$
b_f	Damping coefficient	0.1	N.m.s/rad
d_f	Diameter of fly wheel	0.15	m
c_d	Coefficient of drag	0.26	N/m^2
P	Density of air	1.2	Kg/m^3
r_w	Radius of scooter wheel	0.175	m
μ	Coefficient of viscosity for air	0.03	$N.s/m^2$
d_i	Minimum diameter of primary pulley	0.05	m

In the hybrid mode, the flywheel is coupled to CVT. This hybrid mode is split into a low speed and high speed mode, because of the limited transmission ratio of the CVT. in low speed mode as shown in figure 5 (a,b) the engine shaft 1 is coupled in series with the flywheel shaft (2) to CVT input shaft (3). For the lower speed range, for speeds ranging from 0 to 65 km/hr the fly wheel is used as the main power source for the vehicle. During braking kinetic energy of the vehicle is being recovered in the flywheel. the engine is needed only for short period of time and is shut down and disconnected, when inoperative a wet plate clutch is used as standing device allowing the vehicle to accelerate from standstill.

International Journal of Engineering Research & Technology (IJERT)
ISSN: 2278-0181
Vol. 5 Issue 02, February-2016

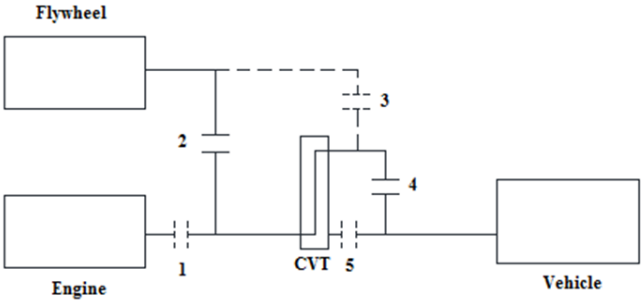

Fig:5 (a) Low speed hybrid mode

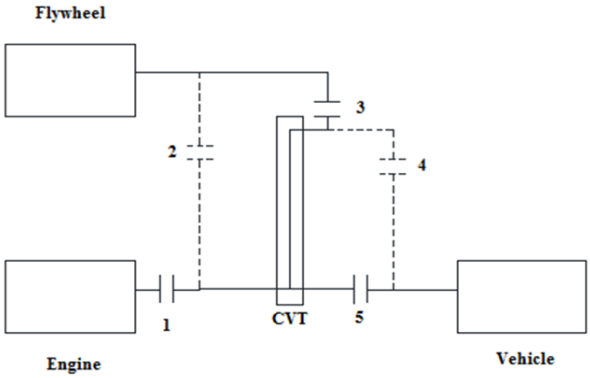

Fig 5 (b) High speed hybrid mode

Figure 7 shows the linear relation between speed ratio and time. In this figure the relation is assumed to be uniform during a period of time 16 s and then to remain constant during a period of time of 5 s.

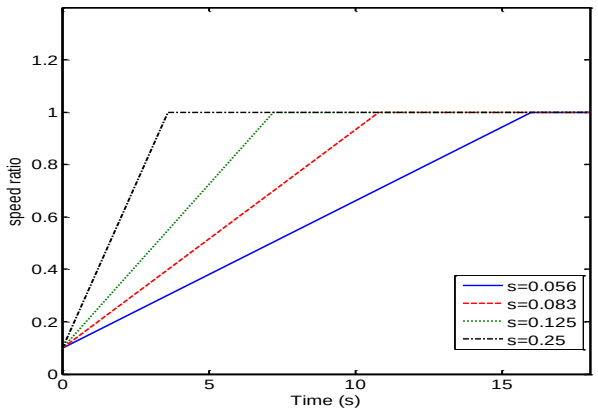

Fig 6 Speed ratio – time relation ship

Fig. 7 shows the speed ratio – time relationship while accelerating and decelerating

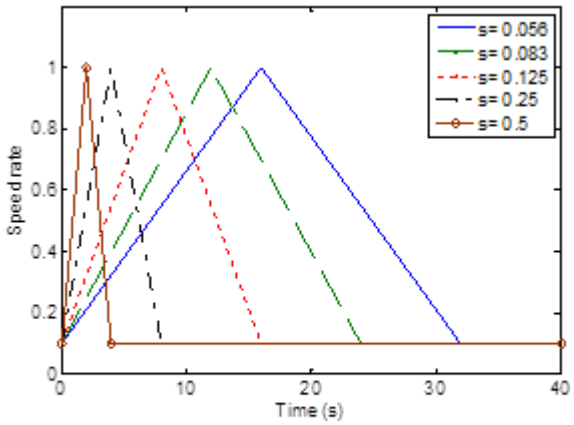

Fig.7 Speed ratio – time relationship (Acceleration - Deceleration)

A-GEOMETRY ANALYSIS

Figure 8 study the relation between speed ratio and inclination angle. From this figure we can see, as the inclination angle is 17° the speed ratio is zero and this angle decreases as the speed ratio increases and reaches to be 1° as the speed ratio is 1.

Figure 9 shows the variation of pulleys radius with time during a period of acceleration and a period of constant velocity. It is clear from this figure that, the radius of primary pulley increases from 0.01m to be 0.05m and the radius of secondary pulley decreases from 0.09m to 0.05m.

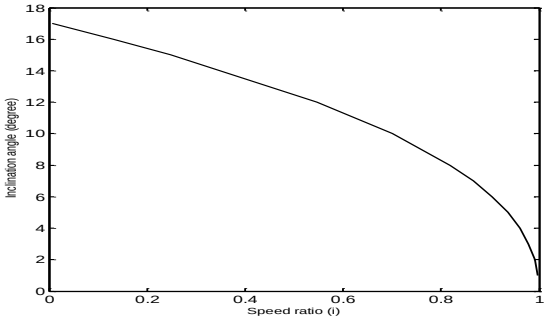

Fig. 8 Relation between speed ratio and inclination angle (δ)

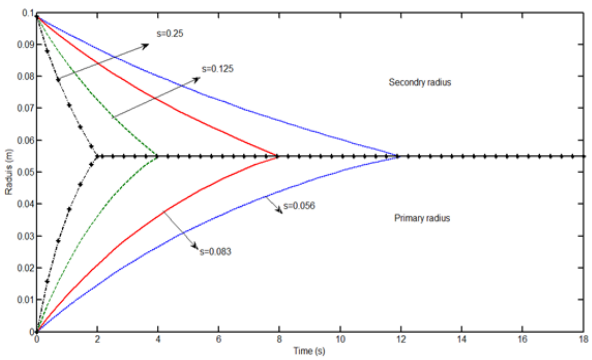

Fig 9: Radius change for different slope

International Journal of Engineering Research & Technology (IJERT)
ISSN: 2278-0181
Vol. 5 Issue 02, February-2016

Also it is seen from this figure that, the variation time of radius change depends on the value of rate acceleration factor, as s changes from 0.056 to 0.25 the time of changing radius varies from 16 sec to be 4 sec. The mechanism of CVT depends on the variation of radial velocity of belt through the pulley which is related to axial velocity of that pulley. The axial velocity is important to change the radius of primary and secondary pulleys.

Figure 10 illustrates the change of radial velocity as the driver becomes to accelerate the scooter. Also four values of rate of acceleration factors is taken in our analysis s = 0.056, 0.083, 0.125 and 0.25. It is clear from this figure that, for secondary pulley the radial velocity increases suddenly at time zero to reach a certain value and then decreases gradually during a certain time which depends on the rate of speed ratio, finally it reaches to a constant value since the velocity of scooter is kept to be constant during the motion. For primary pulley the radial velocity increases with a negative sign suddenly at time zero to a certain value and then decreases gradually during a certain time depends also on the rate of speed ratio before reaching a constant velocity. Also this figure shows that, as the speed ratio rate increases the radial velocity increases and its gradient with time decreases. In most practical application the scooter is driven on different types of roads. The roads may be smooth, rough or irregular type.

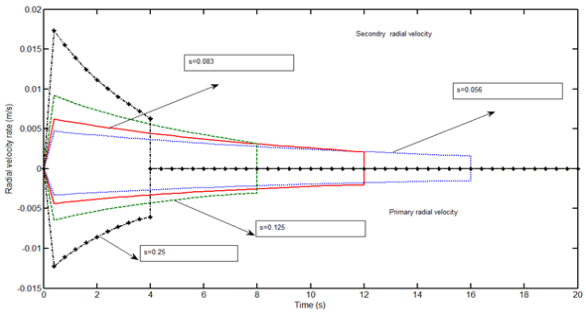

Fig 10 Effect of speed rate on radial velocity

Figure 11 shows the relation between time and axial velocity of primary and secondary pulley during transmission of motion. For different rate of speed ratio it is found from this figure that the axial velocity depends on rate of speed ratio since its minimum value appears at lowest value of rate of speed ratio.

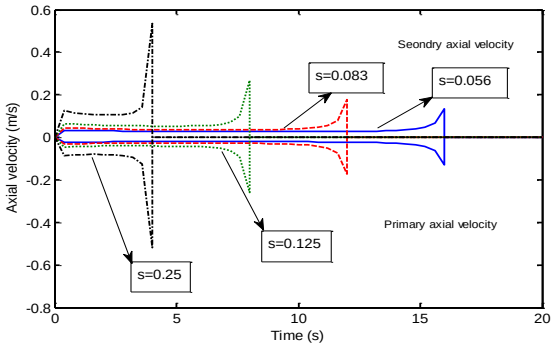

Fig 11: Axial velocity of primary and secondary pulley during transmission of motion

B-DYANAMIC ANALYSIS

Figure 12 shows the variation of primary pulley speed during hybrid mode in which the flywheel is a main source for moving the scooter. In this figure the speed of primary pulley changes from 2000 – 1000 r.p.m. as the speed ratio changes from 0.1 to 1 as mentioned in figure 5(b). Also this relation is illustrated for different rate of speed ratio.

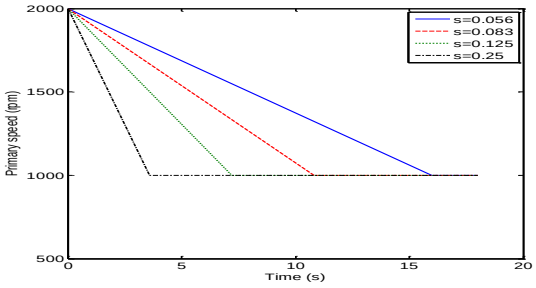

Fig 12.Primary speed vs. time

The dynamic response of drive line as the scooter velocity changes from Zero to 65 km/hr is illustrated by figure 13. The effect of speed ratio rate on dynamic performance of the scooter is important when CVT is used as a mechanism for speed variation. Four values of speed ratio rate is taken into considerations s = 0.25, 0.125, 0.083 and 0.056. It is clear from this figure that, the speed ratio rate is a main factor for smooth and comfortable motion for the driver science as the speed ratio increases a disturbance in the drive line appears and is represented by a mechanical vibration acting on the driving shaft.

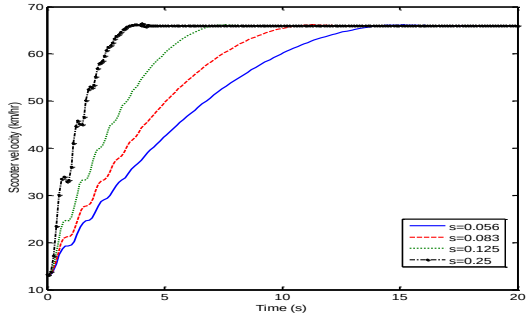

Fig 13 Effect of acceleration rate on scooter velocity c =5 N.m.s/rad

The variation of output torque acting on scooter wheel can be illustrated by figure 14.Also four values of rate of acceleration factor is taken into consideration s = 0.0625, 0.0833, 0.125, 0.25. The velocity of the scooter is assumed to be 65 km/hr which corresponding a max speed in hybrid mode. It is clear from this figure that the torque of drive line fluctuates during a period of time which depends on thevalue of speed ratio rate. Comparing the output torque for different speed ratio rate it is found that, as the speed ratio rate increases the torque fluctuate with high amplitude and its value reaches to 450 N.m as the speed ratio rate is 0.25. As the speed ratio rate is changed to be 0.056 the torque

International Journal of Engineering Research & Technology (IJERT)
ISSN: 2278-0181
Vol. 5 Issue 02, February-2016

fluctuate with maximum value of 160 N.m. the fluctuation time is 3.5s as the speed ratio is 0.25 while while this time is 6s when the speed ratio rate is 0.056.
For s = 0.056 the torque reaches a value of 160N.m in just 0.5 sec and then fluctuates and goes gradually to reach a constant value of 10 N.m/rad after 14 sec. For s = 0.083 the maximum value of torque during acceleration is 180 N.m/rad which can be achieved at 0.5 sec, then its value fluctuates during a period of time 8 sec and after 12 sec is stable.

By making analysis for the results of this figure it is clear that, the rate of speed ratio is a main factor for variation the output torque acting on the wheel and the max value of this torque appears as s = 0.25 and a minimum value at s= 0.056.This indicates that in CVT system rate of speed ratio must be minimum to avoid high fluctuation of torque output to the scooter wheel. This indicates that in CVT system rate of speed ratio must be minimum to avoid high fluctuation of torque output to the scooter wheel.

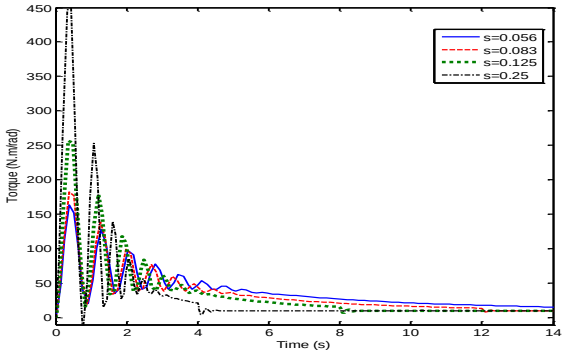

Fig 14: Torque vs. time for different rate of speed ratio

The relation between rate of speed ratio and angular displacement for output shaft (wheel shaft) is shown in figure 15. In this figure effect of maximum torsional damping is studied since four values of damping coefficient, is taken into consideration c_t = 5, 10, 15 and 20 N.m.s/rad.
As seen in this figure the rate of speed ratio is 0.06. The maximum angular displacement is 0.5 rad irrespective the value of torsional damping coefficient. As the rate of speed ratio changes from 0.06 to 0.5 the angular displacement increases for all values of damping coefficient.
As a speed ratio reaches to 0.5 the angular displacement decreases from 2.6 rad to be 2.1 rad as the damping coefficient increases from 5N.m.s/rad to 20N.m.s/rad.
It is important to make analysis for the geometry of CVT components during the rotating motion. As the speed ratio increases the inclination angle δ depends on the speed ratio between primary and secondary pulley.
The time history of angular displacement for output wheel of scooter is shown in figure 16. Different rate of speed ratio is taken into account and its values are (0.056, 0.083, 0.125, and 0.25). It is illustrated by this figure that the angular acceleration fluctuates and its peaks depends on the rate of speed ratio as the rate of speed ratio increases the angular displacement increases to reach a value of 1.55 rad as the rate of speed ratio 0.25 and then the angular displacement is kept to be constant after 4 sec irrespective of rate of speed ratio. For s = 0.25 the time taken to reach the peak of 1.55 rad is about 0.5 sec then it returns to -0.05 rad in about 0.5 sec then reaches a peak of 0.85 rad then return to zero and after 4 sec it is stable at zero. For s = 0.125 the time taken to reach the peak of 0.9 rad is about 0.5 sec then it returns to 0.1 rad in about 0.5 sec then reaches a peak of 0.6 rad then return to 0.1 rad and after 4 sec it is stable at 0.1 rad and decreases gradually to zero after 12 sec. For s = 0.083 the time taken to reach the peak of 0.6 rad is about 0.5 sec then it returns to 0.1 rad in about 0.5 sec then reaches a peak of 0.45 rad then return to 0.1 rad and after 5 sec it is stable at 0.1 rad and decreases gradually to zero after 12 sec. For s = 0.056 the time taken to reach the peak of 0.5 rad is about 0.5 sec then it returns to 0.1 rad in about 0.5 sec then reaches a peak of 0.35 rad then return to 0.1 rad and after 6 sec it is stable at 0.1 rad and decreases gradually to zero after 12 sec.

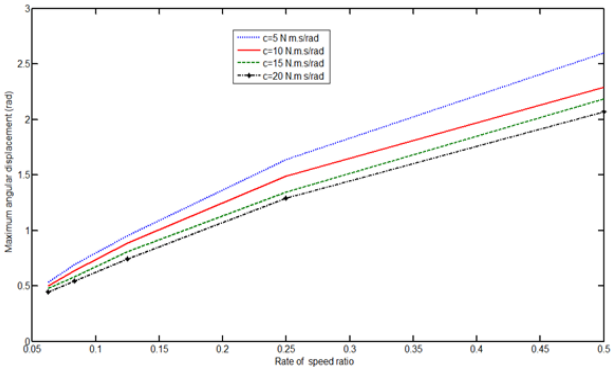

Fig 15 : Relation between rate of speed ratio (ramp effect) on maximum angular displacement of CVT output shaft

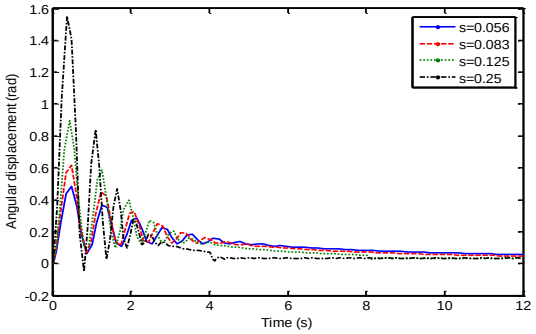

Figure 16: Time history for angular displacement

Fig 17 shows three different loads on the scooter wheel The load acting on the wheel is represented by a friction torque during rolling the scooter wheel

International Journal of Engineering Research & Technology (IJERT)
ISSN: 2278-0181
Vol. 5 Issue 02, February-2016

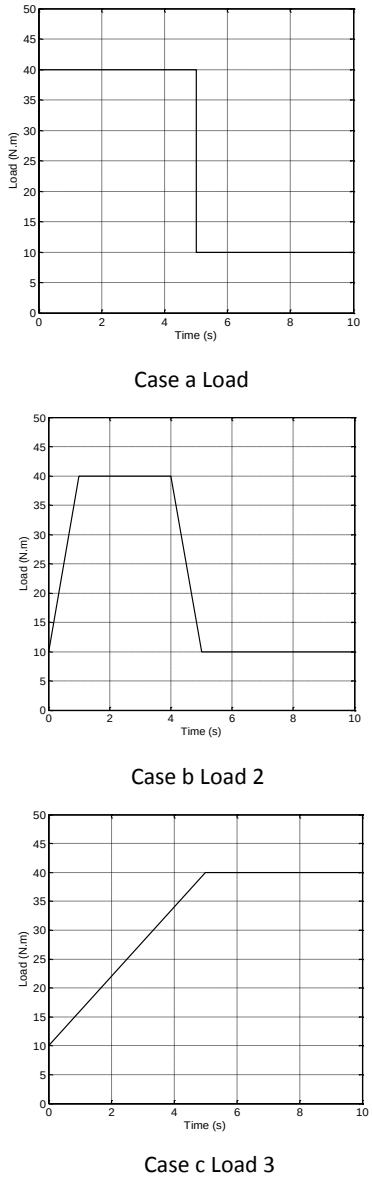

Fig. 17 Effect of different loads on wheel torque

Fig. 18 represents the effect of different loads on the resultant torque acting on the scooter wheel.
I t is clear from this figure that, the torque varies according to the type of road

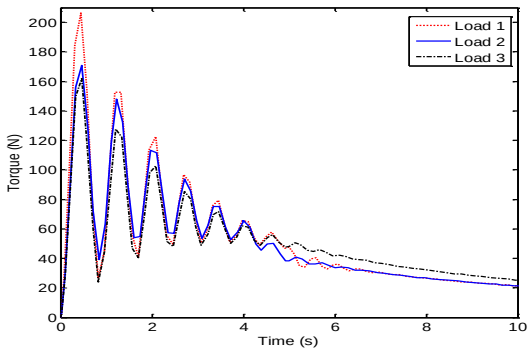

Fig. 18 Loads acting on scooter wheel

Fig.19 shows the effect of speed ratio rate while acceleration and deceleration on scooter velocity at load 1

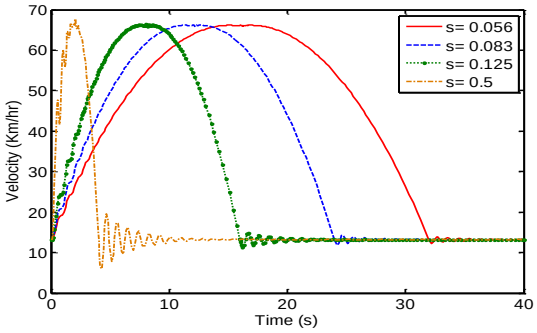

Fig 19 Effect of speed ratio rate (Acceleration - Deceleration) on scooter velocity Load 1

Figure 20 shows the scooter acceleration at load 1

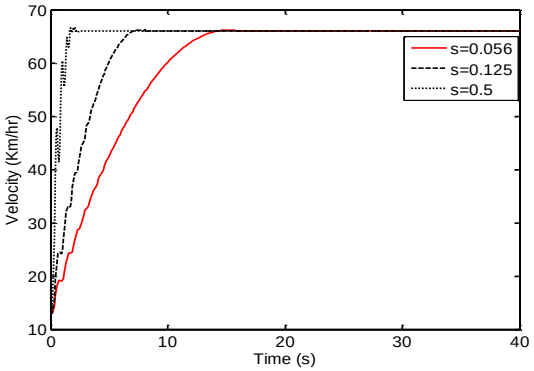

Fig 20 Scooter velocity at high speed rate (Acceleration) load 1

Fig.21 represents the FFT amplitude of wheel shaft twist angle for different speed rate while accelerating

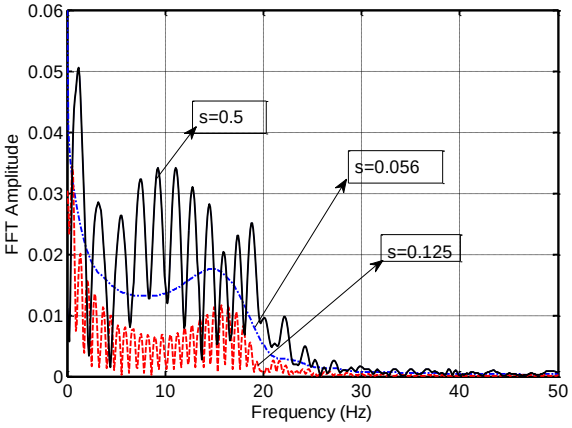

Fig 21 FFT Amplitude of wheel shaft twist angle for different speed rate (acceleration and deceleration Load 1)

International Journal of Engineering Research & Technology (IJERT)
ISSN: 2278-0181
Vol. 5 Issue 02, February-2016

Fig.22 shows the FFT amplitude of wheel shaft twist angle for different speed rate while accelerating and decelerating for load 1

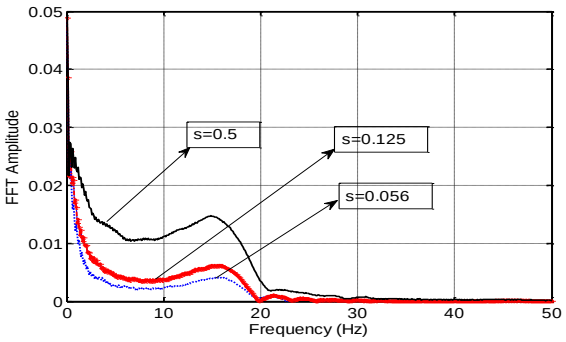

Fig 22 FFT Amplitude of wheel shaft twist angle for different speed rate (acceleration) Load 1

IV.CONCLUSIONS

In this work a CVT model is constructed from primary pulley and secondary pulley which its diameters are changing during the transmission of motion.The equations of motion describes the dynamic response of primary shaft and secondary shaft was derived in addition a mathematical formula for variables which control the change in speed ratio is taken into account. From this work the following conclusions can be obtained:

1-Inclination angle of CVT changes from 17º to 1º as the speed ratio changes from 0 to 1.

2-The radius of primary pulley increases and the radius of secondary pulley decreases during the transmission of motion and its rate depends on the rate of speed ratio.

3-The primary radial velocity increases and the secondary radial velocity decreases during the transmission of motion and its rate depends on the rate of speed ratio.

4-The relation between time and axial velocity of primary and secondary pulley during transmission of motion depends on the rate of speed ratio.

5-Rate of speed ratio is a main factor for changing the response of output shaft (wheel shaft), since as the rate of speed ratio increases a mechanical vibration appears in output shaft.

6-The output torque acting on scooter wheel depends on the rate of speed ratio and its maximum value is estimated by 450 N.m as rate of speed ratio s = 0.25 and minimum torque of 160 N.m when rate of speed ratio s = 0.0625.

7-Torsional damping is a main factor also for changing the maximum angular displacement since damping coefficient changes from 5 N.m.s/rad to 20 N.m.s/rad.

8-The output torque acting on the scooter wheel depends on nature of roads (rough or smooth) since smooth road minimize the output torque acting on scooter wheel.

REFERENCES

[1] Ramnath N. Lyer – Development of high torque C.V.T. fluids. Ethyl Petroleum Additives, inc., Richmond, Virginia, USA 2003
[2] K.G.O.Van De meerakker, P.C.J.N. Rosielle, B. Bonsen,T.W.G.L. Klassen – Design of an electromechanical ratio & clamping force actuator for a metal V-belt type C.V.T. Technische Universiteit Eindhoven 2004
[3] Masahide Fujita, Hisayasu Murakami, Shigeki Okuno, Mitsuhiko Takahashi – Development of 3-D simulation for power transmitting analysis of C.V.T. driven by dry hybrid V-belt. Power train research and development division, Daihatsu Motor Cp., ltd. Power transmission technical research center, Bando Chemical industries, ltd 2004
[4] T.W.G.L.Klassen, B.Bonsen, K.G.O. Van De Meerakker, B.G. Vroemen, M. Steinbuch – Control oriented identification of an electromechanically actuated metal V-belt C.V.T. Eindhoven University of Technology, department of mechanical engineering 2004
[5] Emery Hendriks, Paul Heegde & Tom Van Proijen – Aspects of a metal pushing V-Belt for automotive CVT application. Van Doorne's Transmissie B.V. 1988.
[6] Yoshiaki Kato, Hiroshi Yamashita & Yoshihiro Kono – A study on the torque capacity of belt CVTs. JATCO Ltd 2004.
[7] Cheng Naishi, Zhang Weihua – The match design of the belt type or chain-type CVTs cone discs and flexible members. Northeastern University, extreme Continuously variable transmission Co, ltd. Shenyang Liaoning P.R.China
[8] Keiju Abo, Kazuhiko Sugano,Takashi Shibayama and Koichi Hayasaki – Development of new-generation belt CVTs with high torque capacity for front drive cars. Jatco ltd, Nissan Motor Co., ltd. 2003.
[9] Toru Fujii,Takemasa Kurokawa and Shigeru Kanehara – A study on a metal pushing V-belt type CVT (part 2: Compression force between metal blocks and ring tension) Doshisha University, Honda R. & D Co., ltd.1993.
[10] Shigeru Kanehara, Toru Fujii and Takashi Kitagawa – A study on a metal pushing V-belt Type CVT(part 3: what forces act on metal blocks?) Doshisha University, Honda R. & D Co., ltd.1994.
[11] Takashi Kitagawa, Toru Fujii and Shigeru Kanehara – A study on a metal pushing V-belt type CVT (part 4: forces act on metal blocks when the speed ratio is changing) Doshisha University, Honda R. & D Co., ltd.
[12] Daisuke Kobayashi, Yutaka Mabuchi and Yoshiaki Katoh – A study on the torque capacity of a metal pushing V-Belt for CVTs. Nissan Motor Co., ltd. 1998 Society of Automotive Engineers, inc.
[13] Hiroyuki Yamaguchi, Hiroyuki Nishizawa, Hideyuki Suzuki, Kunihiro Iwatuki and Kazumi Hoshiya – Development of belt μ saturation detection method for V-Belt type CVT. Toyota central R & D Labs, inc. Toyota Motors Co.2004.
[14] Bert Pennings, Mark van Drogen, Arjen Brandsma, Erik van Ginkel and Marlene Lemmens – Van Doorne CVT fluid test: A test method on Belt-pulley level to select fluids for push belt CVT application.Van Doorne's Transmissie / Bosch Group. 2003.
[15] R. Fewkes, J. Gunsing and J. L. Sumiejski – Lubricant as a construction element in the VDT push-belt CVT system. Lubrizol intl. Labs. Van Doorne's Transmissie BV. Lubrizol Corporation.1993.
[16] Kazuma Hatada, Kazuya Okubu, Toru Fujii, Ryuichi Kido and Mitsuhiko Takahashi – An implicit FE analysis of power transmitting mechanism of CVT using a dry hybrid V-Belt. Doshisha univ. Bando Chemical Industries, ltd. 2002 Society of Automotive Engineers, inc.
[17] Koichi Nakazawa, Hideaki Mitsui, Kazuki Kakigawa, Yasyhiro Murakami, Takao Ishikawa and Rika Yauchibara – Performance of a CVT fluid for high torque transmitting belt-CVTs. Showa Shell Sekiyu K.K. Nissan Motor Co., Ltd. 1998 Society of Automotive Engineers, inc.
[18] Roland Möle – Control & operating behavior of continuously variable chain transmissions. Institute of Automotive Engineering Division Mobile Working Machinery (former institute of Agricultural Machinery) Technische Universitat Munchen.2003.

International Journal of Engineering Research & Technology (IJERT)
ISSN: 2278-0181
Vol. 5 Issue 02, February-2016

[19] Siddhart Shastri & Andrew A. Frank - Comparison of energy consumption & power losses of a conventionally controlled C.V.T. with a servo-hydraulic controlled C.V.T. & with a belt & chain as the torque transmitting element. Hybrid Electric Vehicle Center, University of California, Davis, USA. 2004.
[20] Ir. B. penning, Ir. M. D. Tran, Ir. M. Derks, Ir. A. Brandsma, Ir. M. van Schaik, Dr. B. Boulogne, Dr. J. Davidson – New CVT push-belt design featuring a new maraging steel to cover all front wheel drive power train. Van Doorne's Transmissie b. v., Bosch Group, The Netherlands. Imphy Alloy, Arcelor Group, France.
[21] Ichiro Tarutani, Hirofumi Tani, Yuji Nagasawa – Analysis of the power transmission characteristics of a metal V-belt type CVT. 2005.
[22] Nilabh Srivastava, Imtia-ul-Haque – On the operating regime of a metal pushing V-belt CVT under steady state microslip conditions. Department of Mechanical Engineering, Clemson University, Clemson, USA. 2004.